Possible Martensitic Transformation in In$_2$(Mo,W)X (X = Cr, Mn, Fe, Co, and Ni) Heusler Alloys

YING WANG, XIONG YANG* AND YANHONG XUE

College of Science, Civil Aviation University of China, Tianjin 300300, China

Using first-principles density-functional theory, we investigate systematically the structural, magnetic, and mechanical properties of In$_2$(Mo,W)X (X = Cr, Mn, Fe, Co, and Ni) Heusler alloys. All the studied compounds have a regular structure with different magnetic configurations. By calculating the total energy of a martensitic phase with respect to the austenitic phase, a number of new In$_2$-based magnetic shape memory alloys, In$_2$(Mo,W)X (X = Cr, Mn, Fe, and Co), are first predicted to emerge with the tetragonal martensite phase as their ground state. The tetragonal shear modulus and elastic anisotropy ratio of In$_2$(Mo,W)X (X = Cr, Mn, Fe, and Co) alloys also satisfy the criterion of the martensitic phase. Interestingly, all the In$_2$(Mo,W)X (X = Cr, Mn, Fe, and Co) alloys exhibit higher martensitic start temperature and better ductility in comparison with the well-known material Ni$_2$MnGa.

1. Introduction

Magnetic shape memory alloys (MSMAs) are promising candidates for possible practical applications, due to their multifunctionality, such as magneto-strain coupling [1, 2], magneto-caloric coupling [3, 4], magneto-resistance coupling [5, 6], etc. Compared to conventional shape memory alloy, the martensitic phase transition between high temperature cubic structure and low temperature tetragonal structure in MSMA could be driven by the magnetic field. This is the reason for the high actuation frequency of shape memory effect in MSMA. The most-studied prototype MSMA is Ni$_2$MnGa with the stoichiometric composition, which exhibits strong magnetic-field-induced strain effect (10% at 1 T) [1, 2]. However, the low martensitic transformation temperature and poor ductility of Ni$_2$MnGa hinder its technological applications. Much effort has been made to improve the properties of Ni$_2$MnGa, such as replacing Ga by Al, In, and Sn [7], and substituting Mn by Cr and Fe [8–10]. Out of the researchers' expectation, stoichiometric Ni$_2$MnX (X = Al, In, and Sn) do not show martensitic transition. The martensite start temperatures of Ni$_2$CrGa and Ni$_2$FeGa are far below room temperature. The study on MSMA is further extended to magnetic Heusler alloys with a formula X$_2$YZ (X and Y are transition metals, or lanthanides, and Z is from the main group). For instance, Mn$_2$NiGa is reported to be an interesting MSMA because of a high magnetic transition temperature and a 4% magnetic-field-induced strain [11, 12]. Co$_2$MoGa displays both shape memory effect and large spin polarization at the Fermi level [13].

Recently, a new Ga$_2$-based Heusler alloy of Ga$_2$MnNi is predicted to undergo a martensitic transformation at $T_M = 780$ K [14], which is superior to Ni$_2$MnGa. Ga$_2$MnCo is confirmed experimentally to exist with a ferromagnetic state [15]. Considering that In and Ga belong to the same main group, excess In may have the similar effect on the stabilizing of the martensite phase. The study work on In$_2$-based Heusler alloys has not been reported.

In this paper, using density-functional theory based first-principles calculations, we intend to explore novel MSMAs in the Heusler compounds In$_2$(Mo,W)X as X is a 3d transition metal atom from period IV (X being Cr, Mn, Fe, Co, and Ni). The main focus of our study is to determine the probability of a martensitic transformation which is indicative of shape memory behavior, by analyzing magnetic, energetic, and bulk mechanical properties.

2. Method

First-principles calculations have been widely used to study the physical properties of various compounds including the Heusler alloys, perovskite oxide, yttrium orthoaluminate, rhodium silicides, and carbon dioxide [7–26]. To probe the cubic structural ground state and martensitic transition of In$_2$(Mo,W)X (X = Cr, Mn, Fe, Co, and Ni) alloys, we carry out first-principles density-functional calculations with CASTEP code where the plane-wave basis set is implemented [27, 28]. The exchange correlation functional is treated by using the generalized gradient approximation in the Perdew–Burke–Ernzerhof parametrization scheme [29]. Ultrasoft pseudopotentials are employed to depict the interaction between ions and electrons. We use a cut-off energy of 500 eV for the plane wave expansion. The calculations of the total energies for the cubic

———————

*corresponding author; e-mail: x-yang@cauc.edu.cn

phase are performed with a k mesh of $15 \times 15 \times 15$. For the tetragonal phase, we also use the equivalent kind of k mesh. In primitive cells containing two in atoms, one Mo atom and one X atom are considered in the calculation.

3. Results and discussions

3.1. Ground state structure of austenite phase

For the Heusler alloys In₂(Mo,W)X in the cubic phase, two prototypical structure types exist. The so-called "regular" Heusler type is $L2_1$ Cu₂MnAl-type structure which crystallizes in spacegroup $Fm\bar{3}m$ (No. 225). Another prototype named "inverse" type is the Li₂AgSb-type structure with spacegroup $F\bar{4}3m$ (No. 216). The unit cell incorporates four fcc sublattices with Wyckoff positions (1/4, 1/4, 1/4), (3/4, 3/4, 3/4), (1/2, 1/2, 1/2), and (0, 0, 0). For the regular structure, the equivalent positions (1/4, 1/4, 1/4) and (3/4, 3/4, 3/4) are occupied by two In atoms, while (1/2, 1/2, 1/2), and (0, 0, 0) sites are filled with Mo (W) and X atoms. In the inverse structure, four inequivalent positions are occupied with In at (1/4, 1/4, 1/4), Mo (W) at (3/4, 3/4, 3/4), In at (1/2, 1/2, 1/2), and X at (0, 0, 0).

The tetragonal Heusler structure results from elongation or compression of a cubic crystal structure along the z axis. The tetragonal lattice constants a and c can be obtained from the cubic lattice constant a_0, by taking into consideration that the unit-cell volume $V_0 = a_0^3 \approx a^2 c$ is approximately unchanged after tetragonal distortions [12, 13].
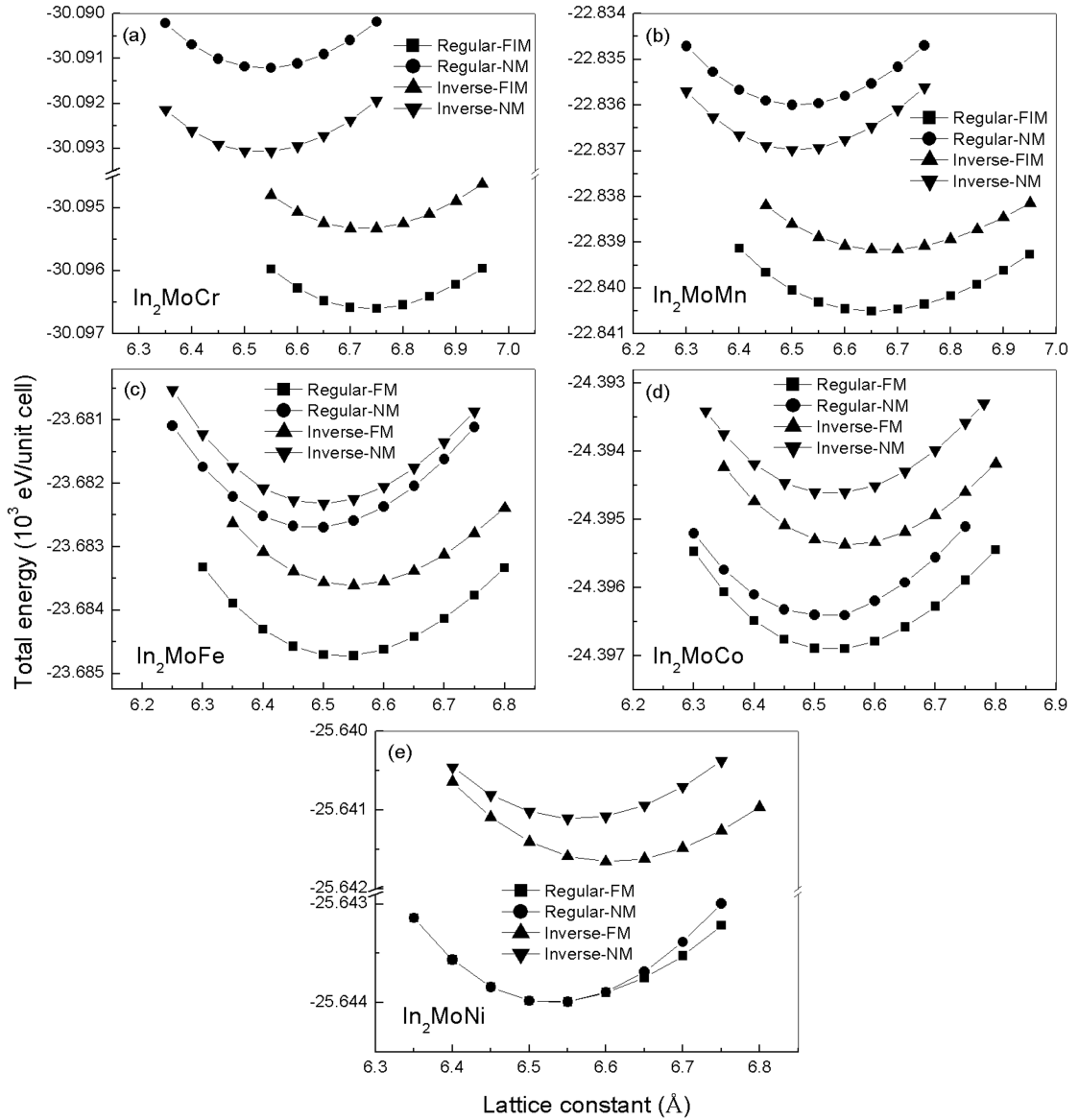

Fig. 1.   Total energies for In₂MoX with X = Cr (a), Mn (b), Fe (c), Co (d), and Ni (e) are plotted against the cubic lattice constants of regular and inverse structures with different magnetic configurations.

To our knowledge, the Heusler alloys $In_2(Mo,W)X$ (X = Cr, Mn, Fe, Co, and Ni) are new unreported materials with no experimental lattice constants. Thus, to determine their cubic ground states in terms of both the crystal structure and the magnetism, we calculate the total energies E_{tot} as functions of lattice constants. Figure 1 displays the results for five In_2MoX alloys. For each compound, we take into account three kinds of magnetic configuration: long-range ferromagnetic (FM), ferrimagnetic (FIM), and nonmagnetic (NM) ordering. A schematic overview of FM and FIM ordering in the regular structure is depicted in Fig. 2. However, the total energies of FM and FIM configurations turn out to be the same for regular structure or inverse structure. As a consequence, only four relation curves are plotted for each alloy in Fig. 1. Our results indicate that for all the cubic compounds $In_2(Mo,W)X$ (X = Cr, Mn, Fe, Co, and Ni), the regular structure always has a lower total energy, instead of the inverse structure. Thus, the ground state of all the cubic $In_2(Mo,W)X$ systems has a regular structure, which agrees well with the results of Ga_2MnNi [14], Ga_2MnCo [15], and Ga_2MoX [16]. In the light of the minimum total energy (see Fig. 1), as well as the moment directions (see Table I), the magnetic configurations of ground states are determined as FIM for $In_2(Mo,W)Cr$ and $In_2(Mo,W)Mn$, FM for $In_2(Mo,W)Fe$ and $In_2(Mo,W)Co$, NM for $In_2(Mo,W)Ni$. In_2MoFe and In_2WMn in the austenite phase have the largest total moment in each series. It is well known that large magnetic moment is beneficial to the application of MSMA. Our obtained equilibrium lattice constants of the cubic alloys $In_2(Mo,W)X$ are listed in Table II. $In_2(Mo,W)X$ (X = Cr and Mn) alloys in FIM state possess a larger lattice parameter than $In_2(Mo,W)X$ (X = Fe, Co, and Ni) in FM or NM state. This may happen because of the decreasing atomic radius of X atoms and the magnetic exchange interaction between Mo (W) and X atoms. In Table II, the well-known material Ni_2MnGa can be also seen as a benchmark, in order to certify the calculation reliability of our method. Our obtained results of Ni_2MnGa are in agreement with previous experiment [30] and calculation [31].
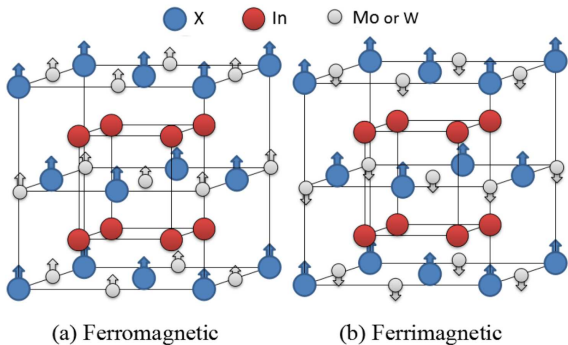

Fig. 2. Parts (a) and (b) present the magnetic orderings for the regular structure, with vectors indicating the orientation of the atomic magnetic moments.

(a) Ferromagnetic   (b) Ferrimagnetic

TABLE I

Magnetic moments for $In_2(Mo,W)X$ (X = Cr, Mn, Fe, Co, and Ni) in the austenite phase. The moments of X and Mo (W) atoms are the first and second values in parentheses, respectively.

Systems	Magnetic configuration	Moment of austenite [μ_B/f.u.]
In_2MoCr	FIM	1.49 (4.67, −3.02)
In_2MoMn	FIM	2.58 (4.12, −1.36)
In_2MoFe	FM	2.72 (2.50, 0.54)
In_2MoCo	FM	2.15 (0.76, 1.75)
In_2MoNi	NM	0 (0, 0)
In_2WCr	FIM	2.35 (4.42, −1.78)
In_2WMn	FIM	2.85 (3.96, −0.89)
In_2WFe	FM	2.39 (2.48, 0.13)
In_2MoCo	FM	1.1 (0.84, 0.38)
In_2MoNi	NM	0 (0, 0)

TABLE II

Calculated lattice constant a_{cub} for the cubic phase, c/a ratios of martensitic transition, energy differences ΔE between the cubic and tetragonal phases, and martensite start temperatures T_M for $In_2(Mo,W)X$ (X = Cr, Mn, Fe, Co, and Ni) and Ni_2MnGa materials.

Systems	a_{cub} [Å]	c/a	ΔE [meV/atom]	T_M [K]
In_2MoCr	6.7359	1.45	33.7	391
In_2MoMn	6.65	1.49	97.1	1126
In_2MoFe	6.5323	1.54	119.4	1385
In_2MoCo	6.5273	1.53	13.3	154
In_2MoNi	6.5277	–	–	–
In_2WCr	6.7187	1.47	94.4	1095
In_2WMn	6.6626	1.51	151.7	1760
In_2WFe	6.5515	1.55	189.6	2199
In_2WCo	6.5409	1.55	110.1	1277
In_2WNi	6.5576	1.45	40.6	471
Ni_2MnGa	5.838	1.28	12.19	141
	5.832^a	1.26^c	6.18^e	72^e
	5.836^b	1.27^d		210^f

[a]Ref. [30], [b]Ref. [31], [c]Ref. [32], [d]Ref. [9], [e]Ref. [8], [f]Ref. [6]

3.2. Prediction of martensitic transformation

The Heusler alloys may have a possible application as a shape memory alloy device, if they undergo a martensite transformation, which is a structural transition from the high-temperature cubic phase to a lower symmetry phase under a certain temperature. For the sake of probing this structural transition in $In_2(Mo,W)X$ (X = Cr, Mn, Fe, Co, and Ni), we compare the total energy of the cubic phase to that of the tetragonal phase with different c/a ratios.

Figure 3 shows the energy difference between the cubic and tetragonal structures. It is found that the ΔE versus c/a plots of In_2MoX (X = Cr, Mn, Fe, and Co) and In_2WX (X = Cr, Mn, Fe, Co, and Ni) reach an energy
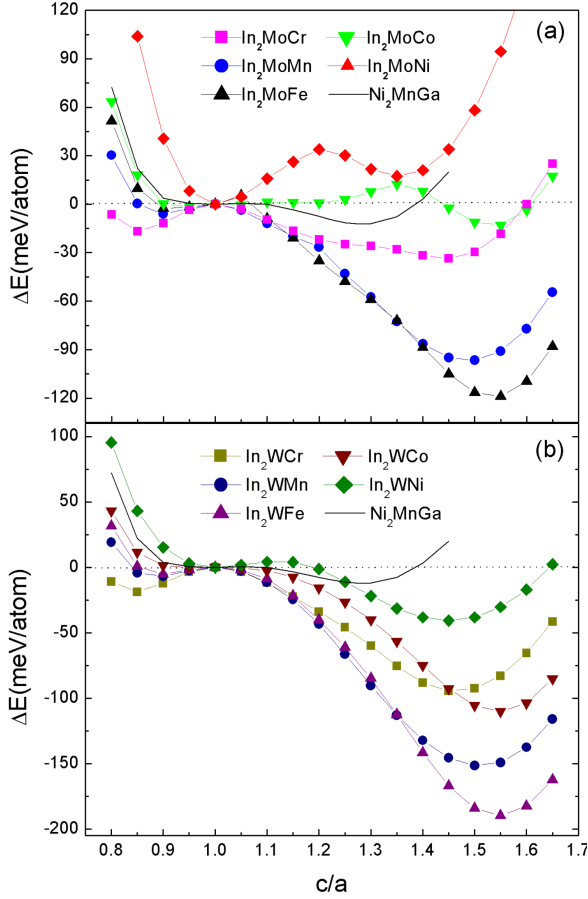
Fig. 3. Total energy difference ΔE between the austenite and the martensite phases as functions of c/a for (a) In$_2$MoX and (b) In$_2$WX (X = Cr, Mn, Fe, Co, and Ni) alloys. The results of Ni$_2$MnGa are used as a benchmark.

minimum smaller than that of the cubic phase. Therefore, all the studied alloys, except for In$_2$MoNi, may possess a tetragonal ground state, and the martensitic phase transition is possible in these materials.

Table II presents the value of c/a and the total energy difference ΔE of tetragonal transition as well as the martensite start temperature T_M for In$_2$(Mo,W)X (X = Cr, Mn, Fe, Co, and Ni) and Ni$_2$MnGa compounds. It can be seen that our tetragonal c/a ratio of Ni$_2$MnGa consists well with prior experimental [32] and theoretical results [9]. The equilibrium values of c/a corresponding to the martensitic transition are bigger than 1.45 for the investigated alloys. In$_2$MoCr and In$_2$WNi have the same value of c/a with Ga$_2$MnV alloy [15]. The total energy differences ΔE of the tetragonal distortion are larger than 13 meV/atom for In$_2$MoX (X = Cr, Mn, Fe, and Co) and In$_2$WX (X = Cr, Mn, Fe, Co, and Ni), which exceeds 12.19 meV/atom of Ni$_2$MnGa. The larger energy difference could power greater driving force to overcome the resistance of martensitic transition. Thus, all the In$_2$MoX (X = Cr, Mn, Fe, and Co) and In$_2$WX (X = Cr, Mn, Fe, Co, and Ni) alloys are expected to undergo

a martensitic phase transition. In addition, it has been verified that the total energy difference ΔE in Ni–Mn–Ga alloys is proportional to the martensitic transition temperature T_M via the equation $\Delta E = k_B T_M$ [8, 13, 14], where k_B is the Boltzmann constant.

It still works for this relationship to evaluate the T_M of other shape-memory alloys TiX (X = Ni, Pd, Pt) [33]. Herein, the calculated T_M of In$_2$MoX (X = Cr, Mn, and Fe) and In$_2$WX (X = Cr, Mn, Fe, Co, and Ni) are above room temperature. The value of T_M for In$_2$MoCo (154 K) almost amounts to 141 K, for Ni$_2$MnGa. It is reported that some high temperature shape memory alloys, whose martensitic transition temperatures are above 393 K, can be applied in engines of turbines, automobiles, and airplanes [34–36]. We must mention that the effect of phonons is neglected in our calculation. This may result in the difference between the estimated phase transition temperatures and the real values of transition temperatures. However, these theoretical data are expected to provide a useful reference for the experiment.

3.3. Bulk mechanical response for martensitic transition

In the following section, we discuss the bulk mechanical properties of In$_2$(Mo,W)X with X = Cr, Mn, Fe, Co, and Ni. The elastic constants C_{ij} of a material can describe the response to an imposed stress on the material. Properties such as the bulk modulus B and the shear modulus G can be computed from the values of C_{ij}. Table III shows the elastic constants and the relevant parameters of In$_2$(Mo,W)X. The calculated values of Ni$_2$MnGa listed in Table III match well with the available theoretical and experimental data of Roy and Chakrabarti [8], Worgull et al. [37], and Stenger and Trivisonno [38].

In$_2$(Mo,W)X alloys in the austenitic phase have only three independent elastic constants: C_{11}, C_{12}, and C_{44}. For a stable cubic structure, the mechanical criteria are as follows: $C_{11} > 0$, $C_{44} > 0$, $C_{11} + 2C_{12} > 0$, and $C_{11} - C_{12} > 0$ [39]. It is found from Table III that all the conditions are satisfied for In$_2$(Mo,W)X (X = Co and Ni) and the last condition is not met for In$_2$(Mo,W)X (X = Cr, Mn, and Fe). This implies that the austenitic phase of In$_2$(Mo,W)X (X = Cr, Mn, and Fe) alloys may be mechanically unstable. We further examine the stability of these materials by investigating the tetragonal shear modulus $C\prime$ and the elastic anisotropy ratio A, which are defined as $C\prime = 0.5 \times (C_{11} - C_{12})$ and $A = C_{44}/C\prime$. The constants $C\prime$ and A linked with phonon modes are indicators of cubic structural stability [13, 40]. If the value of $C\prime$ is negative or close to zero, the cubic structure is mechanically unstable. The larger is the constant A, the more unstable the cubic structure. If the anisotropy ratio A is bigger than 2, the cubic alloys will undergo a tetragonal martensite transformation. For the MSMA Ni$_2$MnGa with a martensite transition, the value of $C\prime$ (2.35) is positive but pretty close to zero, and the value of A (47.4) is far greater than 2. In terms of In$_2$(Mo,W)X (X = Cr, Mn, and Fe), the tetragonal shear modulus $C\prime$ are negative. For In$_2$MoCo and In$_2$WX (X = Co and Ni),

Bulk mechanical properties of the cubic austenite phase of $In_2(Mo,W)X$ (X = Cr, Mn, Fe, Co, and Ni) and Ni_2MnGa materials.

Materials	C_{11} [GPa]	C_{12} [GPa]	C_{44} [GPa]	$C\prime$ [GPa]	B [GPa]	G_V [GPa]	G_R [GPa]	G_V/B
In_2MoCr	77.3	88.6	57.7	-5.65	84.8	32.4	-16.6	0.38
In_2MoMn	92.0	96.9	65.2	-2.45	95.3	38.1	-6.6	0.40
In_2MoFe	114.3	115.1	64.1	-0.4	114.8	38.3	-1.0	0.33
In_2MoCo	132.5	119.6	64.3	6.45	123.9	41.2	14.1	0.33
In_2MoNi	144.9	111.7	62.6	16.6	122.8	44.2	29.6	0.36
In_2WCr	87.6	106.5	63.5	-9.45	100.2	34.3	-30.4	0.34
In_2WMn	90.3	110.1	63.9	-9.9	103.5	34.4	-32.3	0.33
In_2WFe	106.4	121.4	67.6	-7.5	116.4	37.5	-22.6	0.32
In_2WCo	129.6	125.0	72.6	2.3	126.5	44.5	5.5	0.35
In_2WNi	135.9	121.9	53.5	7	126.6	34.9	14.6	0.28
Ni_2MnGa	160.4	155.7	111.3	2.35	157.3	67.7	5.7	0.43
	162.5^a	157.3^a	108.9^a	2.58^a	159^a	66^a	6.2^a	0.42^a
	152^b	143^b	103^b	4.5^b	146^b	64^b	10.6^b	0.44^b
	156^c	143^c	98^c	6.5^c		61^c	14.78^c	

[a]Ref. [8], [b]Ref. [37], [c]Ref. [38]

the value of $C\prime$ is greater than zero, but the anisotropy ratio A is beyond 8. Therefore, the In_2MoX (X = Cr, Mn, Fe, and Co) and In_2WX (X = Cr, Mn, Fe, Co, and Ni) compounds have a mechanically unstable cubic phase, which are expected to transform from austenitic to martensitic phase.

The bulk modulus B is connected with the resistance of the alloy to fracture, while the shear modulus G indicates the resistance to plastic deformation. From the so-called Hill theory [41], the value of G can be obtained from the shear moduli of Voigt (G_V) [42] and Reuss (G_R) [43], which means $G = (G_V + G_R)/2$. As observed for Ni_2MnGa and similar Heusler alloys [13], the experimental value of G is close to the calculated value of G_V, due to the large underestimation of G_R. Following the previous works [8, 13], the G_V value is considered as the shear modulus G. According to Pugh's proposition [44], a low G/B ratio corresponds to ductility, whereas a high value may be related to a more brittle nature. The critical value of G/B between ductility and brittleness is around 0.57. From Table III, it can be found that the G/B ratio of all the $In_2(Mo,W)X$ series is less than 0.4, and lower than that of Ni_2MnGa. The G/B value of In_2WNi (0.28) is minimum in the studied systems, only 49% of 0.57. Thus, all the $In_2(Mo,W)X$ (X = Cr, Mn, Fe Co, and Ni) can be classified as ductile materials. In a word, from magnetic, energetic (Fig. 3), and bulk mechanical properties, $In_2(Mo,W)X$ (X = Cr, Mn, Fe, and Co) compounds are predicted as novel magnetic shape memory alloys.

4. Conclusions

In the research field of magnetic shape memory alloys, the previous studies have paid little attention to the In_2-based Heusler alloys so far. In this paper, we perform first-principles calculations on the structural, magnetic, mechanical properties of the $In_2(Mo,W)X$ (X = Cr, Mn, Fe, Co, and Ni) compounds. Based on the energy stability, magnetism, and mechanical properties, $In_2(Mo,W)X$ (X = Cr, Mn, Fe, and Co) are predicted to exist as new magnetic shape memory alloys. The martensitic transition temperatures of $In_2(Mo,W)X$ (X = Cr, Mn, Fe, and Co) are estimated, which are over room temperature, except for In_2MoCo. The plastic property of $In_2(Mo,W)X$ is found to be superior to Ni_2MnGa. Out of the studied alloys, $In_2(Mo,W)X$ (X = Cr and Mn) are expected to emerge as promising candidates as ferrimagnetic shape memory alloys, and $In_2(Mo,W)X$ (X = Fe and Co) may be applied as ferromagnetic shape memory alloys. This work is the first prediction for physical properties of In_2-based Heusler alloys, which still needs experimental validation.

References

[1] S.J. Murray, M. Marioni, S.M. Allen, R.C. OHandley, T.A. Lograsso, *Appl. Phys. Lett.* **77**, 886 (2000).

[2] A. Sozinov, A.A. Likhachev, N. Lanska, K. Ullakko, *Appl. Phys. Lett.* **80**, 1746 (2002).

[3] T. Krenke, E. Duman, M. Acet, E.F. Wassermann, X. Moya, L. Mañosa, A. Planes, *Nat. Mater.* **4**, 450 (2005).

[4] X. Zhou, W. Li, H.P. Kunkel, G. Williams, *J. Phys. Condens. Matter* **16**, L39 (2004).

[5] S.Y. Yu, Z.H. Liu, G.D. Liu, J.L. Chen, Z.X. Cao, G.H. Wu, B. Zhang, X.X. Zhang, *Appl. Phys. Lett.* **89**, 162503 (2006).

[6] C. Biswas, R. Rawat, S.R. Barman, *Appl. Phys. Lett.* **86**, 202508 (2005).

[7] T. Krenke, M. Acet, E.F. Wassermann, X. Moya, L. Mañosa, A. Planes, *Phys. Rev. B* **73**, 174413 (2006).

[8] T. Roy, A. Chakrabarti, *J. Magn. Magn. Mater.* **401**, 929 (2016).

[9] Y. Qawasmeh, B. Hamad, *J. Appl. Phys.* **111**, 033905 (2012).

[10] M.B. Sahariah, S. Ghosh, C.S. Singh, S. Gowtham, R. Pandey, *J. Phys. Condens. Matter* **25**, 025502 (2013).

[11] G.D. Liu, J.L. Chen, Z.H. Liu, X.F. Dai, G.H. Wu, B. Zhang, X.X. Zhang, *Appl. Phys. Lett.* **87**, 262504 (2005).

[12] S. Singh, M. Maniraj, S.W. D'Souza, R. Ranjan, S.R. Barman, *Appl. Phys. Lett.* **96**, 081904 (2010).

[13] T. Roy, D. Pandey, A. Chakrabarti, *Phys. Rev. B* **93**, 184102 (2016).

[14] S.R. Barman, A. Chakrabarti, S. Singh, S. Banik, S. Bhardwaj, P.L. Paulose, B.A. Chalke, A.K. Panda, A. Mitra, A.M. Awasthi, *Phys. Rev. B* **78**, 134406 (2008).

[15] G.J. Li, E.K. Liu, Y.J. Zhang, Y. Du, H.W. Zhang, W.H. Wang, G.H. Wu, *J. Appl. Phys.* **113**, 103903 (2013).

[16] Y. Wang, X. Yang, Y.H. Xue, Y.F. Chen, *J. Appl. Phys.* **124**, 085112 (2018).

[17] J. Bai, J.M. Raulot, C. Esling, X. Zhao, L. Zuo, *Solid State Phenom.* **160**, 69 (2010).

[18] J. Bai, J.M. Raulot, Y.D. Zhang, C. Esling, X. Zhao, L. Zuo, *J. Appl. Phys.* **109**, 014908 (2011).

[19] C. Lu, J.J. Wang, P. Wang, X.X. Xia, Y.Y. Jin, P.F. Lie, G. Bao, *Phys. Chem. Chem. Phys.* **19**, 1420 (2017).

[20] M. Ju, C. Lu, Y.Y. Yeung, X.Y. Kuang, J.J. Wang, Y.S. Zhu, *ACS Appl. Mater. Inter.* **8**, 30422 (2016).

[21] J.J. Wang, A. Hermann, X.Y. Kuang, Y.Y. Jin, C. Lu, C.Z. Zhang, M. Ju, M.T. Sic, T. Iitaka, *RSC Adv.* **5**, 53497 (2015).

[22] C. Lu, M.S. Miao, Y.M. Ma, *J. Am. Chem. Soc.* **135**, 14167 (2013).

[23] C. Lu, Q. Li, Y.M. Ma, C.F. Chen, *Phys. Rev. Lett.* **119**, 115503 (2017).

[24] C.Z. Zhang, G.L. Sun, J.J. Wang, C. Lu, Y.Y. Jin, X.Y. Kuang, A. Hermann, *ACS Appl. Mater. Interfaces* **9**, 26169 (2017).

[25] C.Z. Zhang, X.Y. Kuang, Y.Y. Jin, C. Lu, D.W. Zhou, P.F. Li, G. Bao, A. Hermann, *ACS Appl. Mater. Interfaces* **7**, 26776 (2015).

[26] L.P. Ding, P. Shao, F.H. Zhang, C. Lu, L. Ding, S.Y. Ning, X.F. Huang, *Inorg. Chem.* **55**, 7033 (2016).

[27] P. Hohenburg, W. Kohn, *Phys. Rev. B* **136**, 864 (1964).

[28] W. Kohn, L.J. Sham, *Phys. Rev.* **140**, A1133 (1965).

[29] J.P. Perdew, K. Burke, M. Ernzerhof, *Phys. Rev. Lett.* **77**, 3865 (1996).

[30] Y.W. Ma, S. Awaji, K. Watanabe, M. Matsumoto, N. Kobayashi, *Solid State Commun.* **113**, 671 (2000).

[31] J.Y. Rhee, Y. Kudryavtsev, J. Dubowik, Y. Lee, *J. Appl. Phys.* **93**, 5527 (2003).

[32] P.J. Brown, A.Y. Bargawi, J. Crangle, K.U. Neumann, K.R.A. Ziebeck, *J. Phys. Condens. Matter* **11**, 4715 (1999).

[33] Y.Y. Ye, C.T. Chan, K.M. Ho, *Phys. Rev. B* **56**, 3678 (1997).

[34] K. Otsuka, X. Ren, *Intermetallics* **7**, 511 (1999).

[35] J.H. Yang, C.M. Wayman, *Intermetallics* **2**, 111 (1994).

[36] J.V. Humbeeck, *J. Eng. Mater. Technol.* **121**, 98 (1999).

[37] J. Worgull, E. Petti, J. Trivisonno, *Phys. Rev. B* **54**, 15695 (1996).

[38] T.E. Stenger, J. Trivisonno, *Phys. Rev. B* **57**, 2735 (1998).

[39] Z. Wu, E.J. Zhao, H.P. Xiang, X. Hao, X.J. Liu, J. Meng, *Phys. Rev. B* **76**, 054115 (2007).

[40] R. Mahlangu, M.J. Phasha, H.R. Chauke, P.E. Ngoepe, *Intermetallics* **33**, 27 (2013) and the references therein.

[41] R. Hill, *Proc. Phys. Soc. A* **65**, 349 (1952).

[42] W. Voigt, *Ann. Phys. (New York)* **274**, 573 (1889).

[43] A. Reuss, *Z. Angew. Math. Mech.* **9**, 49 (1929).

[44] S.F. Pugh, *Philos. Mag.* **45**, 823 (1954).